agriculture

Article

Non-Destructive Quality Evaluation of Tropical Fruit (Mango and Mangosteen) Purée Using Near-Infrared Spectroscopy Combined with Partial Least Squares Regression

Pimpen Pornchaloempong [1], Sneha Sharma [2], Thitima Phanomsophon [2], Kraisuwit Srisawat [1], Wasan Inta [1], Panmanas Sirisomboon [2], Witoon Prinyawiwatkul [3], Natrapee Nakawajana [4], Ravipat Lapcharoensuk [2,*] and Sontisuk Teerachaichayut [5]

[1] Department of Food Engineering, School of Engineering, King Mongkut's Institute of Technology Ladkrabang, Bangkok 10520, Thailand
[2] Department of Agricultural Engineering, School of Engineering, King Mongkut's Institute of Technology Ladkrabang, Bangkok 10520, Thailand
[3] School of Nutrition and Food Sciences, Louisiana State University, Baton Rouge, LA 70803, USA
[4] Department of Engineering, King Mongkut's Institute of Technology Ladkrabang, Prince of Chumphon Campus, Chumphon 86160, Thailand
[5] Department of Food Process Engineering, School of Food-Industry, King Mongkut's Institute of Technology Ladkrabang, Bangkok 10520, Thailand
* Correspondence: ravipat.la@kmitl.ac.th; Tel.: +66-8-4433-1156

check for updates

Citation: Pornchaloempong, P.; Sharma, S.; Phanomsophon, T.; Srisawat, K.; Inta, W.; Sirisomboon, P.; Prinyawiwatkul, W.; Nakawajana, N.; Lapcharoensuk, R.; Teerachaichayut, S. Non-Destructive Quality Evaluation of Tropical Fruit (Mango and Mangosteen) Purée Using Near-Infrared Spectroscopy Combined with Partial Least Squares Regression. *Agriculture* **2022**, *12*, 2060. https://doi.org/10.3390/agriculture12122060

Academic Editors: Ahmed Mustafa Rady, Ewa Ropelewska and Quan-Sheng Chen

Received: 14 October 2022
Accepted: 28 November 2022
Published: 30 November 2022

Abstract: Mango and mangosteen are commercially important tropical fruits with a short shelf life. Fruit processing is one of the alternatives to extend the shelf life of these fruits. Purée is one of the processed products of fresh fruit. In this research, the quality of mango and mangosteen purée was analyzed. Titratable acidity (TA) and total soluble solids (TSS) were predicted using non-destructive near-infrared (NIR) spectroscopy. A partial least squares regression (PLSR) model was developed based on the NIR spectra with a wavelength ranging from 800 to 2500 nm. The PLSR model returned a coefficient of determination (r^2) and a ratio of prediction to deviation (RPD) of 0.955 and 4.7 for TSS, and 0.784 and 2.2 for TA, in the mango purée. Similarly, the best model was selected for the TSS prediction in the mangosteen purée through PLSR, with an r^2, a root mean square error of cross-validation (RMSECV), and RPD of 0.799, 0.3% malic acid, and 2.2, respectively. The results show the possible application of NIR spectroscopy in the product processing line, although a larger number of samples with wide variation in future studies are needed as an input to update the model, in order to obtain a more robust model.

Keywords: mango; mangosteen; purée; near-infrared spectroscopy

1. Introduction

Mango (*Mangifera Indica*) and mangosteen (*Garcinia mangostana*) are famous tropical fruits among the fruits of Southeast Asian countries. Mangosteen is a dark purple to red-purple fruit, and the edible fruit, aril, is white, soft, and juicy, with a sweet, slightly acidic taste and a pleasant aroma [1,2]. Edible mango fruits normally have a light-yellow peel, while the ripe, soft, juicy pulp is darker yellowish with a sweet aroma and taste, although different varieties differ slightly in these properties. Mango and mangosteen are exported either fresh or frozen and as processed products from Thailand. These tropical fruits are perishable and have a short shelf life; however, the shelf life can be extended by using several food processing techniques such as juice processing, concentrating, and drying, which could add value to these fruits and create a new market [1]. Mango and mangosteen purées are modified products from fresh fruits, which have a fine, dense, sticky, uniform texture. The purée of fruits is often used as a raw material for other processed products such as drinks, sauces, ice creams, fruit jams, and dried fruits. The quality of purée is

highly influenced by the genetics of the fruit, storage, cooking parameters, refining, and grinding intensity [3]. Quantification of active biochemical compounds and determination of physicochemical property are highly required for the raw materials and the products of fruits and vegetables. The utilization of fast and accurate tools and techniques for quality evaluation can be implemented throughout the food value chain, which will further provide a huge benefit to the natural food industry [4]. Typically, there are two methods to prepare purée from fresh fruits, i.e., by separating the pulp using a pulper finisher or by centrifugal machines [5], which often use the centrifugal force from a sieve that separates the pulp, seed, and peel, or by using a food cutter [6], whereby the pulp and seed have to be separated before the pulp is fed into the spinning tank with a cutter. Producers of purée around the globe are very concerned regarding the quality of their products, as it directly affects consumer demand. A number of different components such as sugars, acids, starch, pectin, water, and fiber directly or indirectly affect various physical properties such as texture, pH, water activity, viscosity, density, color, specific heat, thermal conductivity, and diffusivity, which affect the stability of the fruit product in terms of both chemical reactions and microbial activity [7,8]. In terms of quality assessment, titratable acidity (TA) and total soluble solids (TSS) are important parameters. TA measures the total acid concentration in a food and is determined by the titration of intrinsic acids with a standard base [9]. The TSS value indicates the sweetness of fresh and processed horticultural food products and is used in laboratories for research and by the industry to determine marketing standards [10]. These parameters are important for increasing consumer demand in the competitive market.

Analytical techniques for measuring the quality of purée during the production process are required for rapid and accurate analysis. Several analytical techniques such as liquid chromatography using separation techniques such as reverse-phase chromatography, ion chromatography, ion exclusion chromatography, refractive index detection, and gas chromatography are commonly used to analyze the quality of and adulteration in fruit purée and juice [11]. Although the accuracy of these techniques is very good, they are time-consuming and require intensive sample preparation in some cases [12]. Near-infrared (NIR) spectroscopy has been used widely for decades as a rapid and accurate alternative method for qualitative and quantitative analysis of the juice of fruits such as satsuma mandarins [13], bayberries [14], apples [15], and grapes [16], as well as of purée such as strawberry, raspberry [17], tomato [18], and apple purée [19].

NIR spectroscopy has been used to investigate the internal quality of mango in terms of TSS, vitamin C, TA, ripening index, dry matter, firmness, skin color, maturity index (I_m), weight loss, peel color, pH, peel electrolyte leakage, total phenolic compounds, total flavonoid compounds, antioxidants, total sugar, and reducing sugar content [20–28], and that of mangosteen in terms of translucent disorder [29,30] and soluble solid content [31,32].

The physicochemical quality of fruit purée can be evaluated using NIR spectroscopy both on the purée itself and the intact fruit. The NIR spectroscopy of fresh fruit juices (orange, apple, grapefruit, grape, pear, pineapple, and sugarcane) [33], a mixture of carbohydrates (glucose, sucrose, starch, and cellulose) and organic acids (citric acid and malic acid) in mango purée [34], antioxidant components in tomato [35,36], purée of clingstone peaches to TSS, TA, pH, and total phenolic compounds [37] were analyzed. The adulteration of apple purée in strawberry and raspberry purée was studied [17,38,39], and the use of the NIR spectra of intact fruit for the prediction of purée quality was reported for apple [19].

Partial least squares regression (PLSR) is a well-known bilinear calibration method that describes the behavior of the response block (Y, dependent variables) as a function of the predictor block (X, independent variables) using data compression to reduce a large number of measured collinear spectral variables to a few orthogonal latent variables (LVs) that describe the maximum covariance between X variables and Y variables [40]. In this research, mango and mangosteen purée qualities were analyzed with respect to TSS and TA. A PLSR model was developed based on the spectra acquired using an FT-NIR spectrometer, accompanied by the reference values of the TSS and TA of mango

and mangosteen purée. PLSR was chosen in this work, as it is most widely used in spectral multivariate calibration analysis and is a perfect combination of multiple linear regression (MLR), canonical correlation analysis (CCA), and principal component analysis (PCA) [41]. Through linear regression, the following can be concluded: MLR, PCR, and PLS are actually connected and coherent; there is a gradually developed course of the linear multivariate calibration; there are weaknesses in the MLR sub-rank inversion; and there is insufficient use of spectral information. PCR uses PCA to decompose the spectral array X and performs MLR regression using the score vector, significantly enhancing the model prediction. Meanwhile, PLSR decomposes the spectra X and concentration Y simultaneously and strengthens the corresponding calculation relationship between the two matrices, ensuring that the best calibration model is established [41]. The summarization of PLSR is similar to that of PCR, which uses the typical features of variable reduction methods as well as an orthogonal space for the regression, thereby avoiding the problems derived from collinearity between variables, but the difference from PCR is that PLSR aims at ensuring that the first few latent variables will contain as much information of predictive use as possible [42].

To date, there have been no reports on NIR calibration models for the prediction of the TSS and TA of pure purées of mango and mangosteen. Therefore, the objective of this work was to develop a rapid essential protocol for evaluation of the TSS and TA of purées of mango and mangosteen. Both mango and mangosteen are the popular and highly favorite fruits in Thailand but with very high yields exceeding consumer demand. Hence, further processing into, for instance, purées, is needed, and NIR spectroscopy can serve as a rapid and accurate method for qualitative and quantitative analysis of the purée quality.

2. Materials and Methods

2.1. Sample Collection

Mahachanok mango fruits were obtained from Chiangmai Fresh Co., Ltd., Chaingmai, Thailand, where the mango trees were grown in Taton Sub-district, Mae Ai District, Chaingmai Province. The fruits were harvested 115–120 days after having flower blooming from the orchards in 2019, totaling 100 kg. The obtained mangosteen fruits at the black maturity level were tree-ripened by the Ta Ma Pla mangosteen community enterprise in Ta Ma Pla Sub-district, Lung Suan District, Chumphon Province, and harvested 90 days after flower blooming in 2019, totaling 100 kg. All samples were transported by a fully covered truck from the orchards to the Factory Classroom, School of Engineering, King Mongkut's Institute of Technology Ladkrabang. After that, they were kept in an open area with good ventilation, where there was no sunlight or rain. The fruits were ripened naturally.

2.2. Purée Production

The preparation of mango and mangosteen purée started by selecting the fruits, which weighed 500–1000 g each, and then cleaning and peeling them. To produce mango purée, the pulps were separated from the seed and blended using the food cutter method with a fruit blender (JTC, model M-800A, Taipei, Taiwan) at a high speed (High) for 25 s. For the mangosteen purée, the pulp finisher method was used, using a fruit juice maker (PHILIPS, model HR1922, Shanghai, China) at a spinning speed level 2 until all of the pulp was separated from the seeds. Figure 1 shows the mango purée (a) and mangosteen purée (b).

The purée was kept in a 100 mL, light-brown glass bottle. Each sample was placed into 2 bottles that were capped with a rubber stopper and screw cap. The bottles were kept at −20 °C for 7 days until they were inspected for quality. Before the NIR scanning of the samples, the bottles were taken out for thawing for 3 to 4 h in order to reach a constant normal temperature (25 °C). In total, 88 sample bottles of mangosteen purée and 96 sample bottles of mango purée were used for this experiment.

(**a**) (**b**)

Figure 1. Mango purée (**a**) and mangosteen purée (**b**).

2.3. Spectra Acquisition

The spectra of the purée were acquired using a Fourier transform (FT) NIR spectrometer (MPA Bruker, Etelingen, Germany). The scanning range used was 12,500–4000 cm^{-1} (800–2500 nm), with a resolution of 16 cm^{-1}. One average spectrum was obtained from an average of 32 scans. Background scanning was carried out by using a reference material made of gold before every single scan. The purée was transferred to a glass vial with a 22 mm diameter and 48 mm height, as a measurement cell. Since glass is fairly transparent in the NIR region, no significant radiation loss from the vial itself that can decrease the signal-to-noise ratio was expected, and the vial used had a flat bottom, meaning that the overall signal-to-noise ratio was not degraded [43]. The purée was then covered with a transfection plate made from stainless steel, which provided a full optical path length of 2 mm, and was scanned.

2.4. Total Soluble Solid and Titratable Acidity Measurement

TSS of the mango and mangosteen purée was measured directly using a digital refractometer (Pal 1, Atago, Tokyo, Japan). Purée samples were dropped directly into the refractometer for the TSS measurement, and the refractometer was calibrated and cleaned after each measurement using distilled water. For the TA content measurement, 5 g of purée was weighed and diluted with 25 mL distilled water. The purée solution was then titrated with sodium hydroxide titrant (0.1 M NaOH) to the equivalence point of the neutralization curve or to a predefined absolute pH endpoint using an auto-titrator (Mettler Toledo, Titrator T50, Greifensee, Switzerland). TSS was measured in %Brix, and TA was measured in % malic acid.

2.5. Repeatability, Reproducibility, and Maximum Coefficient of Determination (R^2_{max})

In order to check the reliability of the scanning and reference laboratory method, a precision test was conducted by measuring the repeatability and reproducibility. The reproducibility of the NIR spectra, which indicates the consistency of the spectrometer and the homogeneity of the sample, can be assessed by scanning the same sample and reloading the sample 10 times for a certain number of samples [44]. Then, absorbance values of any wavenumber can be selected, but in this work, the three selected wavenumbers of 8330 (970), 6900 (1450), and 5154 cm^{-1} (1940 nm), which are the vibration bands of water for each spectrum, were used to determine the standard deviation values of the respective absorbances to indicate the repeatability and reproducibility [45,46].

Similarly, the repeatability of the reference method (Rep) can be defined as the standard deviation of the difference between the repeat measurements of the same sample for a certain number of samples and the total number of samples, which is normally called the standard error of laboratory (SEL). In this experiment, the repeatability quantifies the precision of the reference laboratory analysis for measuring the TA and TSS of the mango and mangosteen purée. The maximum coefficient of determination (R^2_{max}) was calculated to determine the maximum explained variance, which was calculated using the unexplained

variance of the reference laboratory error, where there was no error from the NIR scanning, from sample presentation to NIR. R^2_{max} was calculated using the following equation [47]:

$$R^2_{max} = \frac{SD^2_y - Rep^2}{SD^2_y} \quad (1)$$

where SD_y is the standard deviation of the data of the reference value of the purée sample, and Rep is the repeatability of the reference method. The repeatability of the reference method can indicate whether the reference method should be used or not, and it can also determine if the method should be corrected to reduce the error. R^2_{max} indicates whether the model can be developed by using the data from the reference method or not. The coefficient of determination (R^2) of the regression model will be equal to R^2_{max} only when there is an error in the reference test and there is no error in the NIR spectra acquisition. Using the value of Rep and R^2_{max}, a decision can be made as to whether the model should be developed.

2.6. Data Analysis and Modeling

The model was optimized using OPUS software, version 7.0.129 (Bruker OptikGmbH, Baden-Württemberg, Germany) for PLSR using the cross-validation technique. OPUS offers an optimization option in the calibration process, where it recommends the best combination of wavelength and mathematical pretreatment [44]. Three optimization methods are available for PLSR using OPUS, i.e., NIR, General A, and General B. The optimization process in OPUS was explained through direct communication by Sirinnapa Saranwong, Bruker Optics, Germany, as follows. The full wavenumber range is divided into three sub-wavenumbers, namely, 1, 2, and 3. In General A mode (Gen A), the modeling starts to remove each one: 1 + 2 + 3 (full), 2 + 3 (1 is removed), 1 + 3 (2 is removed), 1 + 2 (3 is removed), 2 (1 and 3 are removed), and 1 (2 and 3 are removed). In General B mode (Gen B), the optimization starts from the individual sub-wavenumber, and then, new sub-wavenumbers are added, and some wavenumbers are repeated: 1, 2, 3, 1 + 2, 2 + 3, 2, 1, 1 + 2 + 3, 2 + 3, 1 + 3, and 1 + 2. In NIR mode, the method is similar to, but not the same as, that of General B mode: 1, 2, 1 + 2, 3, 1 + 3, 2 + 3, 1 + 2 + 3, 1, and 2. If any combination returns the lowest root mean square error of estimation (RMSEE), that region is divided into two sub-wavenumbers again. For example, if the condition of 1 + 2 + 3 is the best result, it would be divided into two regions and examined again. The most robust calibrations are obtained by the combination of the optimum wavelength selection and mathematical pretreatment that provides the lowest error [44]. Spectra with no preprocessing and those with preprocessing through constant straight-line subtraction, vector normalization, min–max normalization, multiplicative scatter correction (MSC), the first derivative, the second derivative, and combination pretreatments, such as first derivative + straight-line subtraction, first derivative + vector normalization, and first derivative + MSC, were used for the development of the PLSR model. The optimum model was selected based on statistical parameters such as the number of latent variables (LVs), coefficient of determination of calibration and prediction by cross-validation (R^2 for calibration and r^2 for prediction by cross-validation), root mean square error of calibration and prediction by cross-validation (RMSEC for calibration and RMSECV for prediction by cross-validation), bias, and the ratio of prediction to deviation (RPD).

3. Results and Discussion

3.1. Spectral Characteristics

Figure 2 shows the average raw spectra of the mangosteen and mango purée. The average spectrum showed some obvious peaks at 10,360, 8380, 6942, 5565, and 5207 cm^{-1} (965, 1193, 1441, 1798, and 1920 nm). In the average spectrum, the water peaks with maxima at 10,360 cm^{-1} (typically around 10,300 cm^{-1}, 970 nm), 8380 cm^{-1} (typically around 8330 cm^{-1}, 1200 nm), 6942 cm^{-1} (typically around 6900 cm^{-1}, 1450 nm), and

5207 cm^{-1} (typically around 5154 cm^{-1}, 1940 nm) seem to be shifted slightly toward higher wavenumbers (lower wavelengths). The absorption of these wavelengths is due to the first, second, and third overtone vibrations of O-H of the water molecules in the purée. Similarly, the absorption at 5565 cm^{-1} (around 1780 nm) corresponds to the first overtone of the C-H stretching of cellulose.

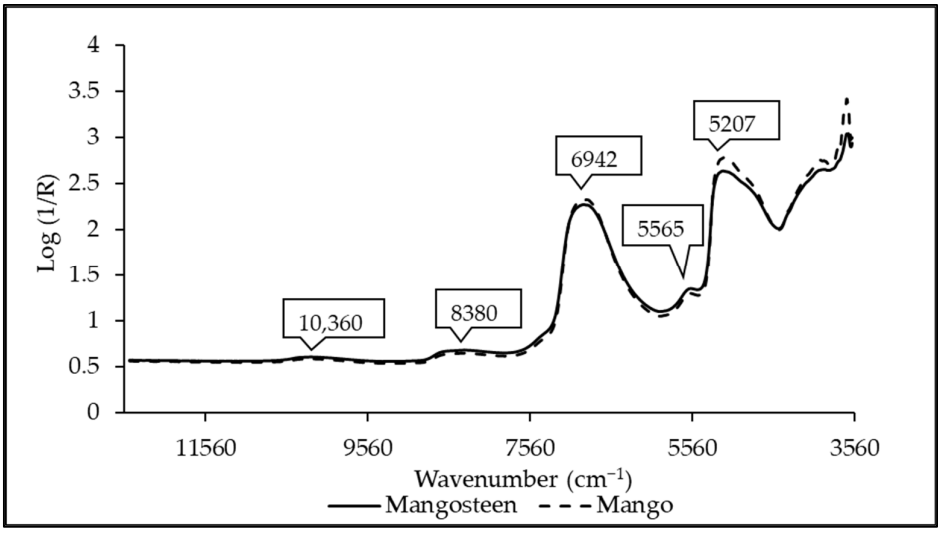

Figure 2. The average raw spectra of mango and mangosteen purée.

3.2. Overall Precision Test

The results of the overall precision test are presented in Table 1. The scanning repeatability values of both the mango and mangosteen purée were 0.0095 and 0.0066, which were lower than the reproducibility values of 0.0237 and 0.0160. In scanning, the repeatability is usually lower than the reproducibility [44]. The reproducibility of the mangosteen purée was lower than that of the mango purée, indicating that the mangosteen purée's texture was more homogeneous. Similarly, the R^2_{max} for the measurement of the TA and TSS of the mango purée was 0.97 and 0.99, which indicates that the error for the reference method for TA and TSS measurement was 3% and 1%. The R^2_{max} values for the measurement of the TA and TSS of the mangosteen purée were 0.70 and 0.94, which indicate that the error for the reference method for TA and TSS measurement was 30% and 6%. Table 1 shows the SD_y and Rep of the reference test. The SD_y and Rep of TA% in the mangosteen purée were low, due to the low $SD_y^2 - Rep^2$, which directly influenced the R^2_{max} in this case. It is possible to increase the R^2_{max} by increasing the range of TA% in mangosteen purée. The results from the precision test show that the NIR model can be developed for the TSS and TA in mango purée and the TSS in mangosteen purée. In a previous study, the repeatability of the measurement of TSS in mango juice squeezed from the pulp was similar to that of the purée, with 0.1 %Brix [48].

Table 1. Repeatability and reproducibility of scanning by FT-NIR, and R^2_{max} of the reference test.

Purée Sample	Scanning		Reference Laboratory			
			TA (%)		TSS (% Brix)	
	Repeatability	Reproducibility	Repeatability	R^2_{max}	Repeatability	R^2_{max}
Mango	0.0095	0.0237	0.008	0.97	0.1	0.99
Mangosteen	0.0066	0.0160	0.001	0.70	0.2	0.94

3.3. Statistical Analysis

The statistical data of the TSS and TA in the mango and mangosteen purée used in the model development are shown in Table 2. In the case of the mango purée, the TSS and TA ranged from about 14.2 to 23.2 %Brix and 0.023 to 0.668%, respectively. The TSS and TA of Nam dok mai si thong' mangoes in different ripening stages in a previous experiment ranged from 7.93 to 8.96 %Brix and from 0.94 to 0.06%, respectively [28]. The difference is due to the fact that the mango fruits used in our experiment were in the stage of complete ripening. In a previous cold chain study, harvested Nam dok mai si thong' mangoes that were submerged in warm water (46 °C) until the middle of the fruit reached the same temperature and kept in a cold room of 20 °C for 7 days, had TSS and TA values of 8.44–17.83 %Brix and 0.73–1.30 g/L, respectively, from day 0 to 7 [49]. The difference is due to the fact that the storage temperature condition was obviously different even though the fruits were harvested at the ripening stage on a commercial harvesting date.

Table 2. Statistical parameters of the mango and mangosteen purée used for model development.

Sample	N	TSS (%Brix)				TA (%)			
		Min	Max	Mean	SD	Min	Max	Mean	SD
Mango	96	14.2	23.2	18.5	2.2	0.023	0.668	0.187	0.104
Mangosteen	88	13.3	16.4	14.8	0.8	0.374	0.573	0.493	0.048

Note: N, number of samples; Min, minimum; Max, maximum; SD, standard deviation.

The range of TSS was 13.3–16.4 %Brix, and that of TA was 0.37–0.57%, for the mangosteen purée. The ranges of TSS and TA in the mangosteen purée were narrow compared to those of the mango purée. These very narrow ranges and very low standard deviations of the TSS and TA of the mangosteen purée led to the low performance of the NIR models. In a previous study, mangosteen fruits were harvested in Chantaburi Province in the east of Thailand at six different maturity stages, and the measurements performed when the fruits of each maturity stage reached stage 6 showed TSS and TA values of 17.2–17.9 %Brix and 0.74–0.81%, respectively [50]. These ranges are different from those values found in our experimental samples due to the different seasons and locations.

3.4. Performance of PLSR Model

The results of the PLSR models for the TSS and TA predictions in the mango and mangosteen purée are shown in Tables 3–6, respectively. All PLSR models for predicting the TSS of the mango purée had a high performance, as shown in Table 3. The best model performance was found for Gen B mode in the spectral ranges of 8046–7151.2 and 6264–5369.2 cm^{-1} (1242–1398 and 1596–1863 nm), with min–max normalization pretreatment. The best prediction result of the TSS in the mango purée produced an r^2 of 0.955, RMSECV of 0.5 %Brix, RPD of 4.7, and bias of −0.01 %Brix. For the TA prediction in the mango purée (Table 4), the suitable wavelengths for PLSR model development were 12,489.5–8925.5 and 8046–5369.2 cm^{-1} (800–1120 and 1242–1863 nm), with multiplicative scatter correction pretreatment. The best model from Gen A presented an r^2 of 0.817, RMESCV of 0.048%, RPD of 2.2, and bias of 0.001% in predicting the TA of the mango purée.

The best model for the TSS prediction in the mangosteen purée was obtained from the optimization method of the NIR mode (Table 5). The PLSR model was developed with spectral ranges of 9403.8–6094.3 and 4605.4–4242.9 cm^{-1} (1063–1640 nm and 2172–2357 nm) without any preprocessing techniques required. The values of r^2, RMSECV, RPD, and bias from the best model for the TSS prediction were 0.799, 0.3, 2.2, and 0.0, respectively. As shown in Table 6, all PLSR models demonstrated a low performance with a low r^2, high RMSECV, and low RPD in predicting the TA in the mangosteen purée. These results indicate that the PLSR model for the TA prediction in the mangosteen purée was not applicable.

Table 3. PLSR models for mango purée TSS prediction.

Model	Spectral Range (cm^{-1})	Pretreatment	LVs	Calibration		Prediction			
				R^2	RMSEC (%Brix)	r^2	RMSECV (%Brix)	RPD	Bias
NIR	9403.8–7498.3 6102–5446.3	Frist derivative + Vector Normalization (17 pts)	5	0.964	0.4	0.939	0.5	4.0	−0.01
Gen A	8933.2–7151.2 6264–5369.2	Vector Normalization	8	0.972	0.4	0.953	0.5	4.7	−0.01
Gen B	8046–7151.2 6264–5369.2	Min–Max Normalization	7	0.965	0.4	0.955	0.5	4.7	−0.01

Table 4. PLSR models for mango purée TA prediction.

Model	Spectral Range (cm^{-1})	Pretreatment	LVs	Calibration		Prediction			
				R^2	RMSEC (%)	r^2	RMSECV (%)	RPD	Bias
NIR	9403.8–7498.3 6102–5446.3	Vector Normalization	7	0.911	0.032	0.780	0.048	2.1	0.001
Gen A	12,489.5–8925.5 8046–5369.2	Multiplicative Scatter Correction	4	0.824	0.045	0.817	0.048	2.2	0.001
Gen B	11,602.3–10,707.5 9828–7151.2 6264–5369.2	Vector Normalization	9	0.976	0.017	0.803	0.046	2.3	0.000

Table 5. PLSR models for mangosteen purée TSS prediction.

Model	Spectral Range (cm^{-1})	Pretreatment	LVs	Calibration		Prediction			
				R^2	RMSEC (%)	r^2	RMSECV (%)	RPD	Bias
NIR	9403.8–6094.3 4605.4–4242.9	No Preprocessing	7	0.875	0.284	0.799	0.3	2.2	0.0
Gen A	11,602.3–10,707.5 8940.9–5369.2	Vector Normalization	10	0.954	0.178	0.746	0.4	2.0	0.0
Gen B	10,715.2–9820.3 8940.9–7151.2 6264–5369.2	Vector Normalization	8	0.941	0.169	0.793	0.3	2.2	0.0

Table 6. PLSR models for mangosteen purée TA prediction.

Model	Spectral Range (cm^{-1})	Pretreatment	LVs	Calibration		Prediction			
				R^2	RMSEC (%Brix)	r^2	RMSECV (%Brix)	RPD	Bias
NIR	9403.8–6094.3 4605.4–4242.9	Frist derivative + Straight-line Subtraction (17 pts)	9	0.662	0.03	0.273	0.048	1.2	−0.001
Gen A	12,489.5–11,602.3 10,715.2–8925.5 5376.9–4482	Constant Offset Elimination	1	0.153	0.05	0.111	0.048	1.2	0.000
Gen B	9828–7151.2	Vector Normalization	7	0.723	0.03	0.248	0.046	1.2	0.000

Until now, there have been no reports on NIR calibration models for the prediction of the TSS and TA of pure purées of mango and mangosteen. Theanjumpol et al. [34]

investigated the characteristic absorption bands for the mixture of carbohydrates (glucose, sucrose, starch, and cellulose) and organic acids (citric acid and malic acid) in mango purée using NIR spectra in the absorption band of 550 to 1100 nm. A PLS model was developed, providing an r^2 of 0.99 and standard error of prediction (SEP) of 0.42%, 0.37%, 0.23%, 0.19%, 0.34%, and 0.26% for glucose, sucrose, starch, cellulose, citric acid, and malic acid, respectively, where the model's performance was better than ours for TSS and TA. This might be because our models were used for predicting the mixed constituents dispersion, but those of Theanjumpol et al. were used for predicting the specific constituent of mango purée. Amodio et al. [37] evaluated the application of the FT-NIR technique (12,500–4000 cm^{-1}) to the purée of clingstone peaches in a glass Petri dish, and a single spectrum was acquired to predict soluble solids (SSC), titratable acidity (TA), pH, and total phenolic compounds. The best results were observed for soluble solids, with a coefficient of determination of 0.841 and an RMSECV of 0.454 %Brix, while lower accuracy was found for flesh phenols, followed by acidity and pH, with an R^2 of 0.529, 0.441, and 0.332, respectively. Szuvandzsiev et al. [35] and Cozzolino [36] reported the estimation of antioxidant components in tomato by combining visible (VIS) and NIR spectroscopy (500 and 1000 nm). The spectra were directly acquired from the fruit purée of five different tomato varieties using a handheld spectrometer, and PLS models were developed in order to predict soluble solids, lycopene, and polyphenols, in which an R^2 and RMSECV of 0.77 and 0.55 %Brix, 0.75 and 1.99%, and 0.72 and 7.63% were obtained, respectively, which were not better than those of Theanjumpol et al. [34].

However, the adulteration of apple purée in strawberry and raspberry purée, not the constituents, was studied by Contal et al. [17] using raw intact fruit (not purée) spectra in the range of 400–2500 nm combined with SIMCA, providing a fair to very good accuracy of 79.07–94.77%, and with PLSR, providing a correlation coefficient (r) of 0.98–0.99 for determining adulteration levels. Downey and Kelly [38] used a standard normal variate (SNV) and the Savizky–Golay second derivative in the range of 400–2498 nm combined with SIMCA, providing a 75.1–95.1% accuracy and with PLSR, providing an r of cross-validation of 0.90 [39]. Besides the use of the spectra of intact fruit for the prediction of purée quality, Lan et al. [19] developed PLS models, in which a good ability to estimate purée characteristics from spectra acquired from corresponding apples, such as viscosity ($R^2 > 0.82$), cell wall content ($R^2 > 0.81$), dry matter ($R^2 > 0.83$), soluble solid content ($R^2 > 0.80$), and TA ($R^2 > 0.80$), was obtained, confirming that the physicochemical quality of fruit purée can be evaluated using NIR spectroscopy both on the purée itself and the intact fruit.

Better predicted models of TSS could be obtained from thin, less opaque fresh fruit juices such as orange, apple, grapefruit, grape, pear, pineapple, and sugarcane than the purée due to no obstruction of fiber-related matter in the juice. This is confirmed by the NIR transmittance juice spectra of orange, apple, grapefruit, grape, pear, pineapple, and sugarcane in the range from 1000 to 2500 nm, with absorbance at 2270 nm, which was found to be a dominant factor in estimating %Brix values in the fruit juices. With the single-wavelength (2270 nm) universal calibration equation, an r^2 of 0.982, SEC = 0.518 %Brix, SEP = 0.621 %Brix, and bias = 0.025 %Brix were found for the fresh fruit juices, and the results were validated using fresh juices of cantaloupe, papaya, and peach, enhancing the applicability to other fruit juices and confirming the reliability of the universal calibration equation [33].

The results of the statistical analysis of the observed and predicted values from the PLSR model for the TA prediction in mangosteen purée are provided in Table 7. The results from the *t* test showed a *p* value of 0.823, which is greater than 0.05; thus, the means of the observed TA by the reference lab method and the predicted TA from the NIR spectra were not significantly different, with a confidence interval of 95%. The results here show that the predicted values and observed values were close, and the RMSECV was low, at 0.0408% (Table 6); therefore, it is possible that the model performance can be improved by increasing the range of TA% and by adding more samples in the model.

Table 7. Result of *t* test: paired sample test for observed and predicted TA% in mangosteen purée.

	Mean (%)	Variance (%)	Pearson Correlation	*p*-Value (Two-Tailed)
Observed TA%	0.495	0.002	0.588	0.823
Predicted TA%	0.499	0.002		

Scatter plots of the PLSR model of the TSS of the mango and mangosteen purée and TA of the mango purée from the cross-validation are shown in Figure 3. The values of the slope of these plots ranged from 0.9986 to 1, indicating the extremely high potential effectiveness of the calibration, where the rate of change in the measured constituents (TSS and TA) is a function of the rate of change in the predicted constituents [44]. Williams et al. found that if the slope is within 0.05 of 1.00, slope adjustment will not improve the data very much, but in practical terms, if the slope differs from 1.00, e.g., by ±0.85 to ±1.15 or by an even greater deviation, this means that the calibration will be affected by slope correction; however, slope correction is not recommended [44]. Figure 3 shows a slope of 0.9986 to 1, and an offset (intercept) of the plots of 0.00 (%Brix or % for TSS and TA, respectively), indicating the extremely high potential effectiveness of the calibration.

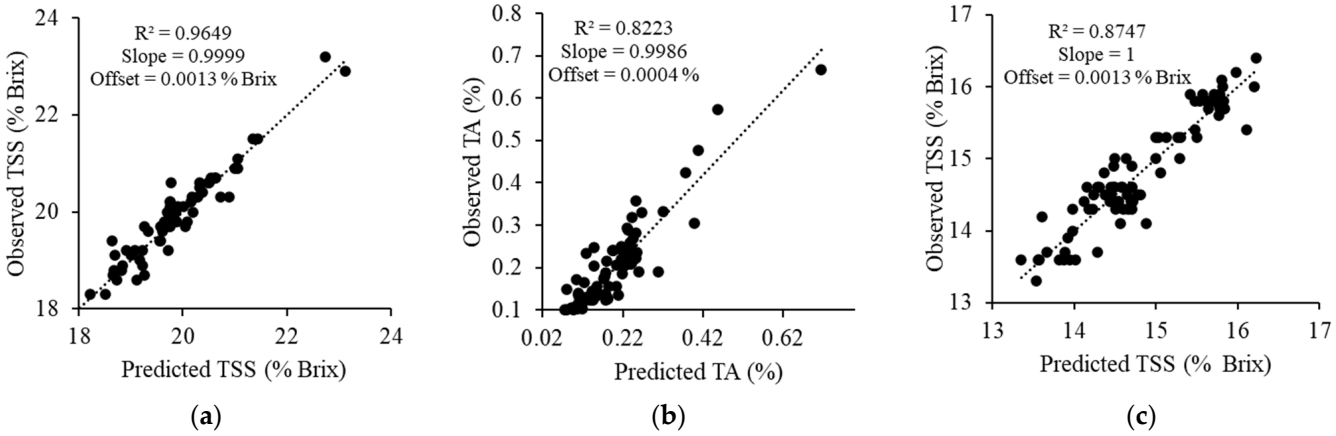

Figure 3. Scatter plots of predicted vs. observed TSS and TA of mango purée by PLSR (**a**,**b**) and TSS of mangosteen purée by PLSR (**c**).

The results from the PLSR model were better for the TSS prediction of the mango and mangosteen purée, with a high r^2 and low RMSECV. The model developed for the TA prediction of the mangosteen purée was not acceptable. The reason for the poor performance of the model is the narrow range of TA for the calibration set. The model could be better if more samples were to be added and if the range of TA could be increased. The mango purée PLSR model for the TSS prediction could be used for most applications, including quality assurance [44]. The PLSR models for the prediction of TA in the mango purée and TSS in the mangosteen purée are acceptable for screening and some other approximate calibrations [44]. The selection of the wavelength range could be an important factor to develop a more robust model for predicting the TSS and TA of mango and mangosteen purée.

3.5. Regression Coefficient and X-Loading

Figures 4–9 show the regression coefficient and X-loading plots of the best model obtained by PLSR. High positive or negative values of the regression coefficient and X-loading weight show the vibration of the band at a particular wavenumber/wavelength that has an influence on the TSS and TA prediction. As most of the variance is explained by the first three LVs, the X-loading plot shows LV1, LV2, and LV3 of the optimum PLSR model. Tables 8–13 show the absorption bands with high regression coefficients and X-loading

weights in the model of the TSS and TA of the mango purée and TSS of the mangosteen purée.

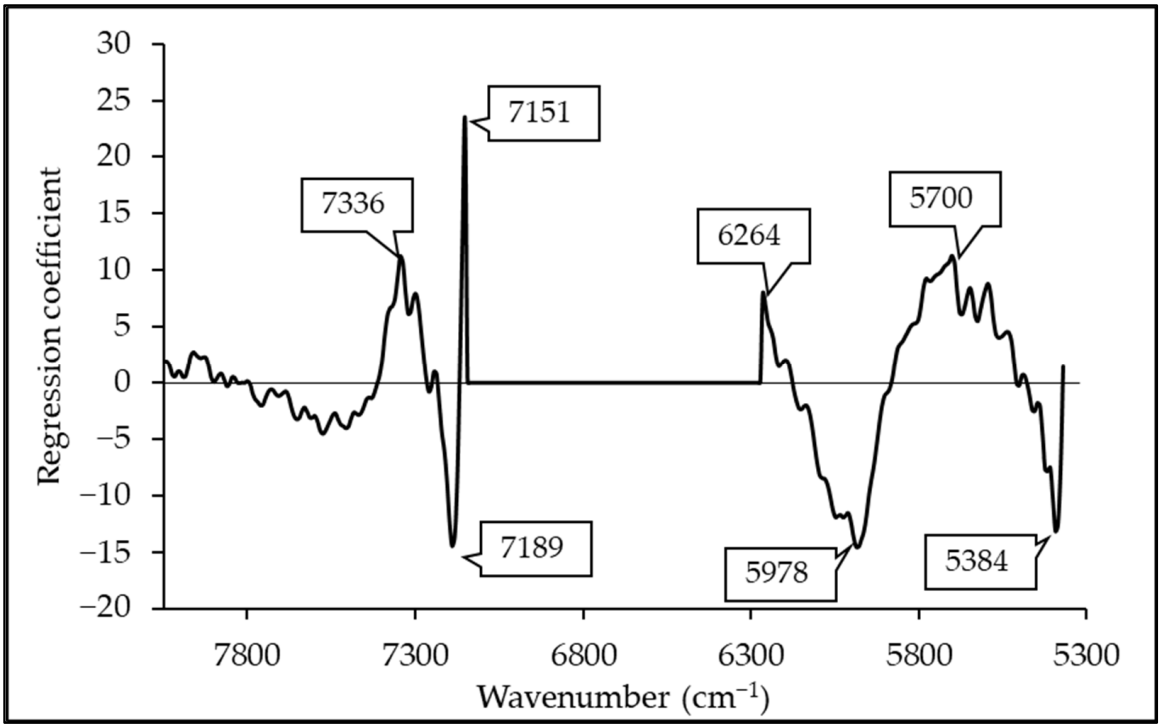

Figure 4. Regression coefficient plot of the PLSR model for TSS prediction in mango purée.

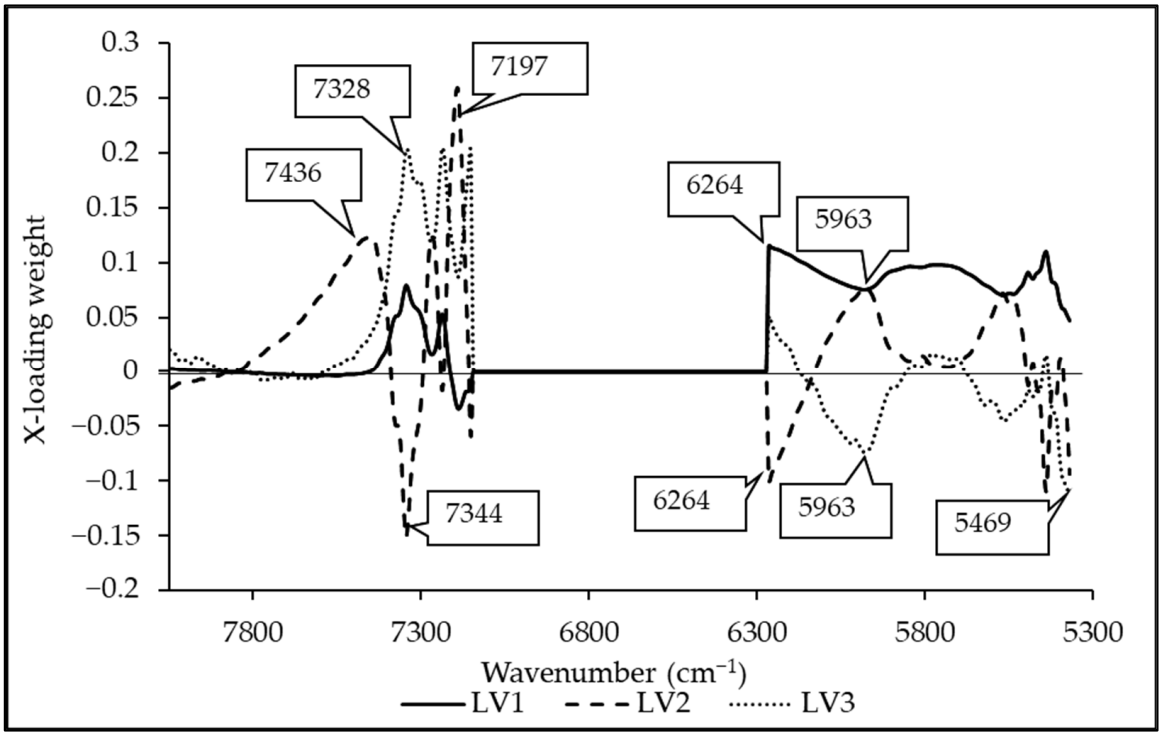

Figure 5. X-loading plot of the PLSR model for TSS prediction in mango purée.

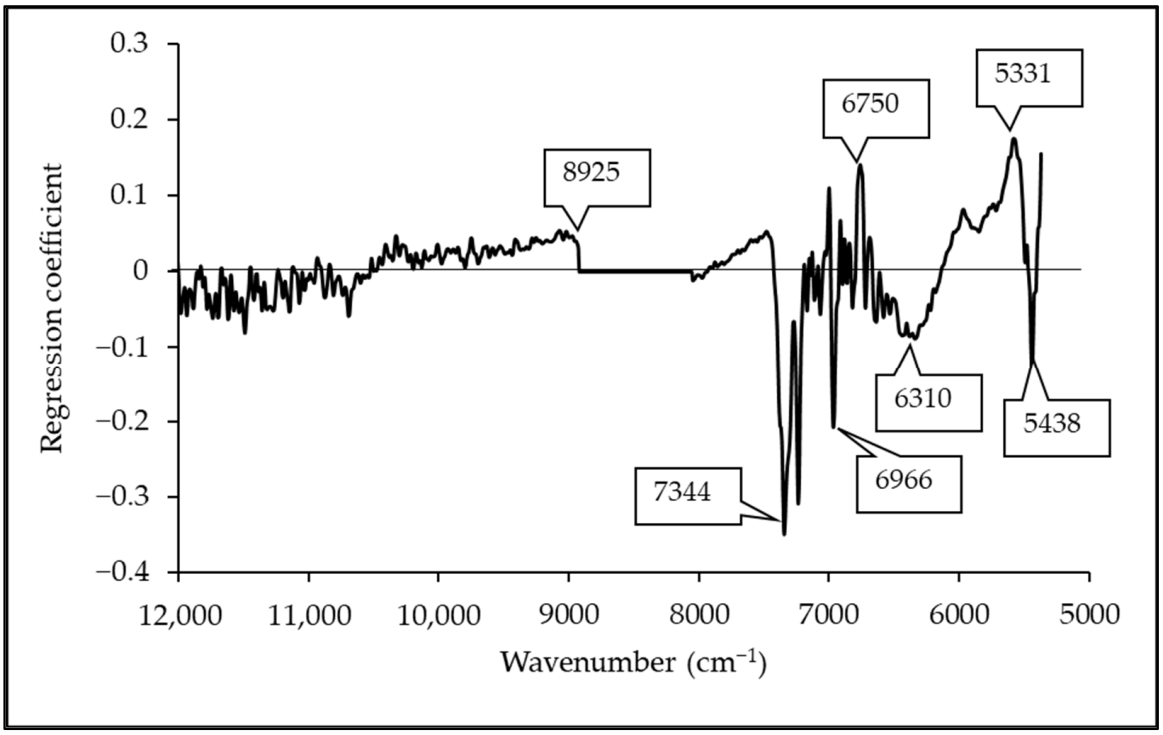

Figure 6. Regression coefficient plot of the PLSR model for TA prediction in mango purée.

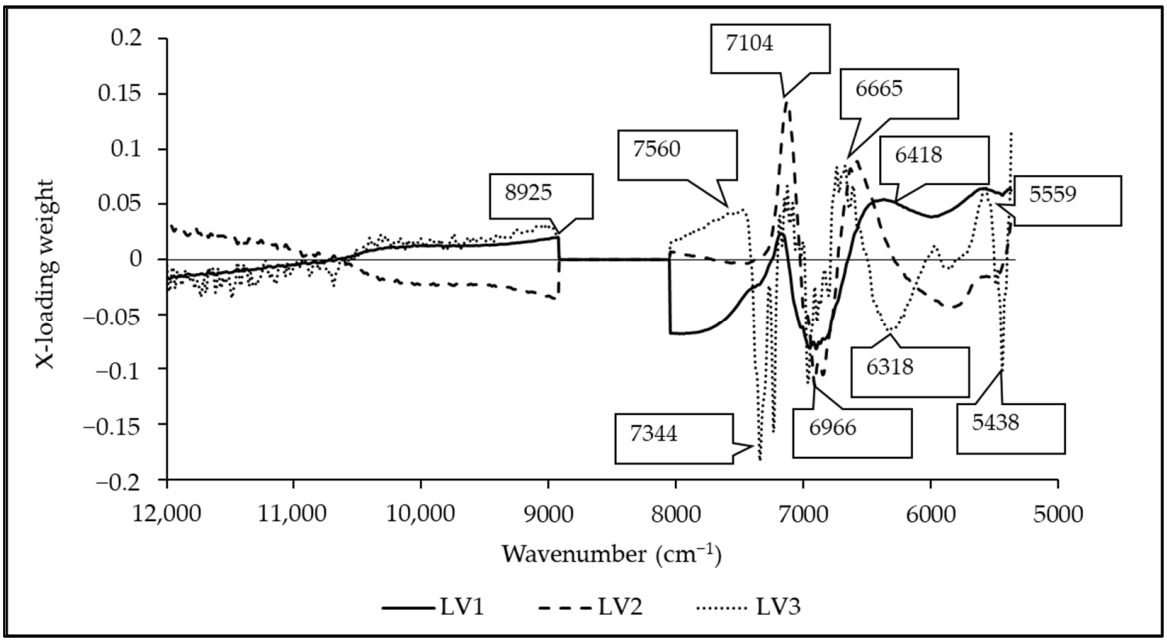

Figure 7. X-loading plot of the PLSR model for TA prediction in mango purée.

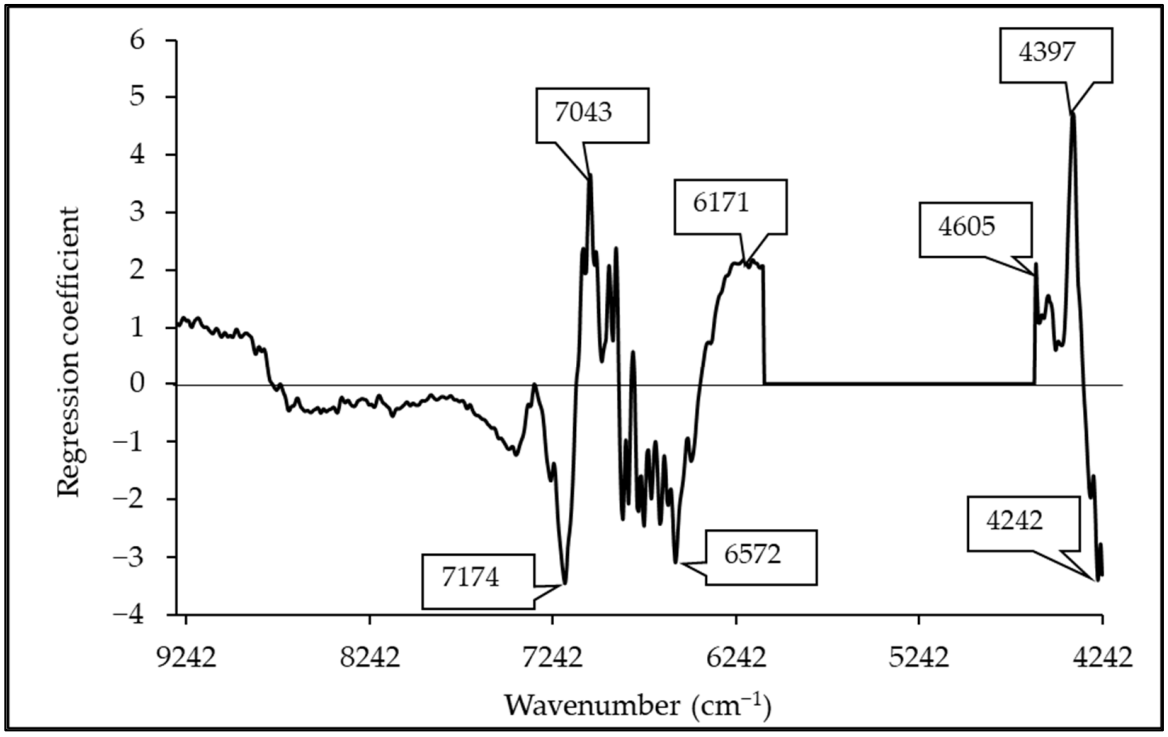

Figure 8. Regression coefficient plot of the PLSR model for TSS in mangosteen purée.

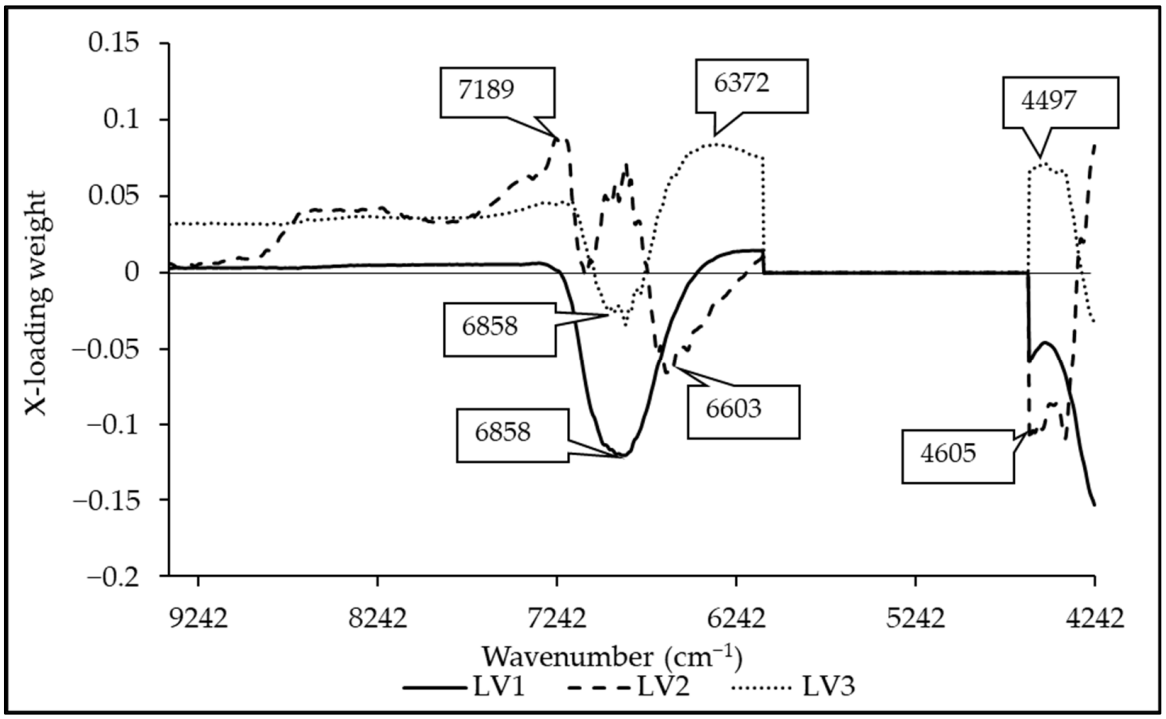

Figure 9. X-loading plot of the PLSR model for TSS in mangosteen purée.

In Figure 4, for the TSS prediction in the mango purée, high-regression coefficient peaks can be seen at 7336, 7189, 7151, 6264, 5978, 5700, and 5392 cm^{-1} (1362, 1391, 1395, 1596, 1673, 1754, and 1857 nm), which might correspond to the bond vibration of CH_3 (1360 nm), CH_2, (1395 and 1765 nm), starch (1900 nm), glucose (1580 nm), and aromatics (1685 nm) [51]. Similarly, from the X-loading weight (Figure 5), it was found that the vibration band of

cellulose at 5960–5438 cm^{-1} (1685–1820 nm; Table 9) showed an important contribution to the TSS prediction of the mango purée.

Table 8. The bands with a high regression coefficient of the PLSR model for TSS in mango purée.

Wavenumber (cm^{-1})	Wavelength (nm)	Referred Wavelength (nm)	Bond Vibration/Functional Group (Structure)	Ref.
7336	1363	1360	2 × C-H str. + C-H def. (CH_3)	[51]
7189	1391	1395	2 × C-H str. + C-H def. (CH_2)	[51]
6264	1596	1580	O-H str. first overtone (starch/glucose)	[51]
5978	1673	1685	C-H str. first overtone (aromatics)	[51]
5700	1754	1765	C-H str. first overtone (CH_2)	[51]
5384	1857	1900	O-H str. + 2 × C-O str. (starch)	[51]

Table 9. The bands with a high X-loading weight of the PLSR model for TSS in mango purée.

Wavenumber (cm^{-1})	Wavelength (nm)	Referred Wavelength (nm)	LVs	Bond Vibration/Functional Group (Structure)	Ref.
7436	1345	1360	2	2 × C-H str. + C-H def. (CH_3)	[51]
7328	1365	1360	2	2 × C-H str. + C-H def. (CH_3)	[51]
7344	1362	1360	1, 3	2 × C-H str. + C-H def. (CH_3)	[51]
7197	1389	1395	2	2 × C-H str. + C-H def. (CH_2)	[51]
6264	1596	1580	1, 2, 3	O-H str. first overtone (starch, glucose)	[51]
5963	1677	1685	3, 2	C-H str. first overtone (aromatics)	[51]
5469	1828	1820	2	O-H str. + 2 × C=O str. (cellulose)	[51]
5438	1839	1820	3	O-H str. + 2 × C=O str. (cellulose)	[51]

According to Theron and Lues (2007), an organic acid is an organic compound with acidic properties that contains carbon, as with all organic compounds [52]. The most common organic acids such as malic acid, citric acid, acetic acid, and formic acid are the carboxylic acids whose Tas are associated with their carboxyl group, –COOH. In Figure 6, for the TA prediction in mango purée, important wavelengths were the vibration band of O-H stretching due to carboxyl acid at 8925 cm^{-1} (1127 nm) [27], the C-H combination of CH_3 at 7344 cm^{-1} (1360 nm), and C=O from saturated and unsaturated carboxyl acid at 6966 cm^{-1} (1437 nm) [53]. The peaks that appear at about 5562 and 5438 cm^{-1} (1780 and 1850 nm) were due to the combination of the C-H stretching + C-H bending of formic acid and the acid chloride second overtone [54]. Other dominant peaks were seen in the X-loading plot (Figure 7) at the wavelengths of 1220, 1315, 1410, 1500, and 1580 nm, which might be monomeric carboxylic acids observed in the gaseous state associated with combinations between the first overtone of the OH stretch and a COH bending mode (1220 nm), and the O-H str. first overtone and OCO bending (1315 nm) [54]. Similarly, bands associated with the O-H str. first overtone of ROH (1410 nm), O-H str. first overtone of starch (1500 nm), and O-H combination of starch and glucose (1580 nm) [51] were confirmed. Figures 6 and 7 show that the wavelength range from 8000 to 5300 cm^{-1} (1449–1887 nm) had a significant effect on the TA prediction, compared to the range from 12,000 to 8000 cm^{-1}. According to Oliveira et al. (2014), the regression coefficients obtained for the NIR spectra of citric acid and malic acid showed strong peaks between 1100 and 1600 nm (9100–6250 cm^{-1}) [55], and according to Xie et al. [56], this spectral region is the most important for the prediction of organic acids [56].

Table 10. The bands with a high-regression coefficient of the PLSR model for TA in mango purée.

Wavenumber (cm^{-1})	Wavelength (nm)	Referred Wavelength (nm)	Bond Vibration/Functional Group (Structure)	Ref.
8925	1120	1127	O-H from carboxyl acid	[53]
7344	1362	1360	2 × C-H str. + C-H def. (CH_3)	[51]
6966	1436	1437	C=O from saturated and unsaturated carboxyl acid	[53]
6750	1481	1480	O-H str. first overtone (glucose)	[51]
6302	1587	1607	C-O from COOH	[53]
5562	1798	1780	C-H combination of formic acid	[54]
5438	1839	1850	Acid chloride	[54]

Most of the important wavelengths in the PLSR model for the TSS prediction in the mangosteen purée were due to the combinations and overtones of bands associated with CH_2 (7174 cm^{-1} (1395 nm), 7043 cm^{-1} (1420 nm), and 6171 cm^{-1} (1620 nm)), starch (6572 cm^{-1} (1522 nm) and 4397 cm^{-1} (2276 nm)), and cellulose (4242 cm^{-1} (2352 nm)) (Figure 8). Similarly, in the X-loading weight plot (Figure 9), peaks related to water at 1450 nm, starch and glucose at 1580 nm, and carbohydrate at 2200 nm [44] were seen, which were the important peaks for the TSS prediction in the mangosteen purée.

Table 11. The bands with a high X-loading weight of the PLSR model for TA in mango purée.

Wavenumber (cm^{-1})	Wavelength (nm)	Referred Wavelength (nm)	LVs	Bond Vibration/Functional Group (Structure)	Ref.
8925	1120	1127	1, 2, 3	O-H from carboxyl acid	[53]
8046	1243	1220	1	O-H str. first overtone	[54]
7560	1323	1315	3	O-H str. first overtone	[54]
7344	1362	1360	3	2 × C-H str. + C-H def. (CH_3)	[51]
7104	1408	1410	1, 2, 3	O-H str. first overtone (ROH)	[51]
6966	1436	1437	1, 2, 3	C=O from saturated and unsaturated carboxyl acid	[53]
6665	1500	1500	2, 3	O-H str. first overtone (starch)	[44]
6481	1543	1540	1	O-H str. first overtone (starch)	[51]
6318	1583	1580	3	O-H str. first overtone (starch and glucose)	[51]
5559	1799	1780	2	C-H combination of formic acid	[54]
5438	1839	1850	2	Acid chloride	[54]

Table 12. The bands with a high-regression coefficient of the PLSR model for TSS in mangosteen purée.

Wavenumber (cm^{-1})	Wavelength (nm)	Referred Wavelength (nm)	Bond Vibration/Functional Group (Structure)	Ref.
7174	1394	1395	2 × C-H str. + C-H def (CH_2)	[51]
7043	1420	1415	C-H str. first overtone (CH_2)	[51]
6572	1522	1528	O-H str. first overtone (starch)	[51]
6171	1620	1620	C-H str. first overtone (CH_2)	[51]
4605	2172	2170	C-H combination (alkenes)	[51]
4397	2274	2276	O-H str. + C-C str. (starch)	[51]
4242	2357	2352	C-H def. second overtone (cellulose)	[51]

Table 13. The bands with a high X-loading weight of the PLSR model for TSS in mangosteen purée.

Wavenumber (cm^{-1})	Wavelength (nm)	Referred Wavelength (nm)	LVs	Bond Vibration/Functional Group (Structure)	Ref.
7189	1391	1395	2	2 × C-H str. + C-H def. (CH_2)	[51]
6858	1458	1450	1, 2, 3	O-H str. first overtone (H_2O)	[51]
6603	1514	1520	2	O-H str. first overtone ($CONH_3$)	[51]
6372	1569	1580	3	O-H str. first overtone (starch and glucose)	[51]
4605	2172	2170	1, 2	C-H combination (alkenes)	[51]
4497	2224	2200	3	C-H str. + C-O str. (carbohydrate)	[44]

4. Conclusions

The application of FT-NIR spectroscopy to predict the total soluble solids (TSS) and titratable acidity (TA, in % malic acid) in mango and mangosteen purée was presented in this research, and the rapid essential protocol starting from mango and mangosteen fruit sample collection, purée preparation, purée sampling and NIR purée spectrum acquisition and to NIR spectroscopy calibration methodology and validation was established. The PLSR model yielded an r^2 and RPD of 0.955 and 4.7 for TSS, and 0.817 and 2.2 for TA, in the mango purée. Similarly, the PLSR model for the prediction of TSS in the mangosteen purée obtained an r^2 and RPD of 0.799 and 2.2. The statistical results show that the PLSR model for the TA% prediction in mangosteen purée must be updated by adding more samples and by increasing the standard deviation of the samples. Since the standard deviation for TA was very low, the PLSR model was not applicable for the TA prediction in the mangosteen purée. Furthermore, in this research, more samples could have been added to perform the test set validation for the PLSR model development. A more robust model can be developed in the future by increasing the range of the prediction parameters that directly affect the performance of the overall model.

Author Contributions: Conceptualization, P.P., P.S. and R.L.; methodology, S.S., T.P., W.I., P.S. and R.L.; software, S.S. and T.P.; validation, S.S., P.S. and R.L.; formal analysis, S.S., T.P., P.S. and R.L.; investigation, S.S., T.P., P.S. and R.L.; resources, P.P., W.I., S.S., T.P., P.S. and R.L.; data curation, S.S. and T.P.; writing—original draft preparation, S.S., T.P., P.S., N.N. and R.L.; writing—review and editing, W.P., P.P., P.S. and R.L.; visualization, S.S., K.S. and T.P.; supervision, P.P., P.S., S.T., N.N. and R.L.; project administration, S.S. and T.P.; funding acquisition, P.P., P.S. and R.L. All authors have read and agreed to the published version of the manuscript.

Funding: This research was funded by the King Mongkut's Institute of Technology Ladkrabang (A118-01162-015) research fund. The APC was funded by the School of Engineering, King Mongkut's Institute of Technology Ladkrabang.

Institutional Review Board Statement: Not applicable.

Informed Consent Statement: Not applicable.

Data Availability Statement: Not applicable.

Acknowledgments: The researchers would like to express their gratitude to Nithiya Rattanapanon, Postharvest Technology Research Center, Faculty of Agriculture, Chiang Mai University, for her advice on the sample collection method.

Conflicts of Interest: The authors declare no conflict of interest.

References

1. Chaovanalikit, A.; Mingmuang, A.; Kitbunluewit, T.; Choldumrongkool, N.; Sondee, J.; Chupratum, S. Anthocyanin and total phenolics content of mangosteen and effect of processing on the quality of mangosteen products. *Int. Food Res. J.* **2012**, *19*, 1047–1053.
2. Martin, F.W. Durian and mangosteen. In *Tropical and Subtropical Fruits: Composition, Properties and Uses*, 1st ed.; Nagy, S., Shaw, D.E., Eds.; AVI Publishing Co., Inc.: Westport, CT, USA, 1980; pp. 407–414.

3. Lan, W.; Bureau, S.; Chen, S.; Leca, A.; Renard, C.M.G.C.; Jaillais, B. Visible, near- and mid-infrared spectroscopy coupled with an innovative chemometric strategy to control apple puree quality. *Food Control* **2021**, *120*, 107546. [CrossRef]
4. Cozzolino, D.; Phan, A.; Netzel, M.; Smyth, H.; Sultanbawa, Y. Monitoring two different drying methods of Kakadu plum puree by combining infrared and chemometrics analysis. *CYTA J. Food* **2021**, *19*, 183–189. [CrossRef]
5. Rattanapaskorn, S.; Rakmae, S. Study on parameters of centrifugal pulping machine for sugar apple. In Proceedings of the 54th Kasetsart University Annual Conference, Bangkok, Thailand, 2–5 February 2016.
6. Jomduang, S.; Chanrittisen, T. Production of Kaew Mango Pulp and quality during storage. In Proceedings of the 37th Kasetsart University Annual Conference, Bangkok, Thailand, 3–5 February 1999.
7. Manohar, B.; Ramakrishna, P.; Ramteke, R.S. Effect of pectin content on flow properties of mango pulp concentrates. *J. Texture Stud.* **1990**, *21*, 179–190. [CrossRef]
8. Tansakul, A.; Kantrong, H.; Saengrayup, R.; Sura, P. Thermophysical properties of papaya puree. *Int. J. Food Prop.* **2012**, *15*, 1086–1100. [CrossRef]
9. Tyl, C.; Sadler, G.D. pH and Titratable Acidity. In *Food Analysis part of Food Science Text Series*, 1st ed.; Nielsen, S.S., Ed.; Springer: Cham, Switzerland, 2017; pp. 389–406.
10. Magwaza, L.S.; Opara, U.L. Analytical methods for determination of sugars and sweetness of horticultural products—A review. *Sci. Hortic.* **2015**, *184*, 179–192. [CrossRef]
11. Dasenaki, M.E.; Thomaidis, N.S. Quality and authenticity control of fruit juices-a review. *Molecules* **2019**, *24*, 1014. [CrossRef]
12. Rodriguez-Saona, L.E.; Fry, F.S.; McLaughlin, M.A.; Calvey, E.M. Rapid analysis of sugars in fruit juices by FT-NIR spectroscopy. *Carbohydr. Res.* **2001**, *336*, 63–74. [CrossRef]
13. Masithoh, R.E.; Haff, R.; Kawano, S. Determination of soluble solids content and titratable acidity of intact fruit and juice of satsuma Mandarin using a hand-held near infrared instrument in transmittance mode. *J. Near Infrared Spectrosc.* **2016**, *24*, 83–88. [CrossRef]
14. Xie, L.; Ye, X.; Liu, D.; Ying, Y. Quantification of glucose, fructose and sucrose in bayberry juice by NIR and PLS. *Food Chem.* **2009**, *114*, 1135–1140. [CrossRef]
15. Włodarska, K.; Khmelinskii, I.; Sikorska, E. Evaluation of quality parameters of apple juices using near-infrared spectroscopy and chemometrics. *J. Spectro.* **2018**, *2018*, 5191283. [CrossRef]
16. Caramês, E.T.S.; Alamar, P.D.; Poppi, R.J.; Pallone, J.A.L. Rapid Assessment of Total Phenolic and Anthocyanin Contents in Grape Juice Using Infrared Spectroscopy and Multivariate Calibration. *Food Anal. Methods* **2017**, *17*, 1609–1615. [CrossRef]
17. Contal, L.; León, V.; Downey, G. Detection and quantification of apple adulteration in strawberry and raspberry purées using visible and near infrared spectroscopy. *J. Near Infrared Spectrosc.* **2002**, *10*, 289–299. [CrossRef]
18. Davies, A.M.C.; Dennis, C.; Grant, A.; Hall, M.N.; Robertson, A. Screening of tomato purée for excessive mould content by near infrared spectroscopy: A preliminary evaluation. *J. Sci. Food Agric.* **1987**, *39*, 349–355. [CrossRef]
19. Lan, W.; Jaillais, B.; Leca, A.; Renard, C.M.G.C.; Bureau, S. A new application of NIR spectroscopy to describe and predict purees quality from the non-destructive apple measurements. *Food Chem.* **2020**, *310*, 125944. [CrossRef]
20. Munawar, A.A.; Suhandy, D. Fast and contactless assessment of intact mango fruit quality attributes using near infrared spectroscopy (NIRS). *IOP Conf. Ser. Earth Environ. Sci.* **2021**, *644*, 012028.
21. Nghiệm, N.; Lộc, N.; Dũng, N.; Ngôn, N. A review on fruit quality assessment by non-destructive methods. *TNU J. Sci. Technol.* **2021**, *226*, 158–167. [CrossRef]
22. Rungpichayapichet, P.; Mahayothee, B.; Nagle, M.; Khuwijitjaru, P.; Müller, J. Robust NIRS models for non-destructive prediction of postharvest fruit ripeness and quality in mango. *Postharvest Biol. Technol.* **2016**, *111*, 31–40. [CrossRef]
23. Anderson, N.T.; Walsh, K.B.; Subedi, P.P.; Hayes, C.H. Achieving robustness across season, location and cultivar for a NIRS model for intact mango fruit dry matter content. *Postharvest Biol. Technol.* **2020**, *168*, 111202. [CrossRef]
24. Mishra, P.; Woltering, E.; El, N. Improved prediction of 'Kent' mango firmness during ripening by near-infrared spectroscopy supported by interval partial least square regression. *Infrared Phys. Technol.* **2020**, *110*, 103459. [CrossRef]
25. Taira, E.; Nakamura, S.; Hiyane, R.; Honda, H.; Ueno, M. Development of a nondestructive measurement system for mango fruit using near infrared spectroscopy. *Eng. Appl. Sci. Res.* **2017**, *44*, 189–192. Available online: https://ph01.tci-thaijo.org/index.php/easr/article/view/97562 (accessed on 22 November 2022).
26. Jha, S.N.; Narsaiah, K.; Jaiswal, P.; Bhardwaj, R.; Gupta, M.; Kumar, R.; Sharma, R. Nondestructive prediction of maturity of mango using near infrared spectroscopy. *J. Food Eng.* **2014**, *124*, 152–157. [CrossRef]
27. Sharma, S.; Sirisomboon, P.; Pornchaloempong, P. Application of a Vis-NIR spectroscopic technique to measure the total soluble solids content of intact mangoes in motion on a belt conveyor. *Hortic. J.* **2020**, *89*, 545–552. [CrossRef]
28. Tangpao, T.; Phuangsaujai, N.; Kittiwachana, S.; George, D.R.; Krutmuang, P.; Chuttong, B.; Sommano, S.R. Evaluation of Markers Associated with Physiological and Biochemical Traits during Storage of 'Nam Dok Mai Si Thong' Mango Fruits. *Agriculture* **2022**, *12*, 1407. [CrossRef]
29. Teerachaichayut, S.; Kil, K.Y.; Terdwongworakul, A.; Thanapase, W.; Nakanishi, Y. Non-destructive prediction of translucent flesh disorder in intact mangosteen by short wavelength near infrared spectroscopy. *Postharvest Biol. Technol.* **2007**, *43*, 202–206. [CrossRef]
30. Terdwongworakul, A.; Nakawajana, N.; Teerachaichayut, S.; Janhiran, A. Determination of translucent content in mangosteen by means of near infrared transmittance. *J. Food Eng.* **2012**, *109*, 114–119. [CrossRef]

31. Teerachaichayut, S.; Terdwongworakul, A.; Phonudom, J.; Uamsatianporn, W. The robustness of PLS models for soluble solids content of mangosteen using near infrared reflectance spectroscopy. *Fresh Prod.* **2009**, *3*, 60–63.
32. Janhiran, A.; Thanapase, W.; Kasemsumran, S.; Teerachaichayut, S. Using near infrared spectroscopy techniques for non-destructive determination of total soluble solids in mangosteen fruits. In Proceedings of the 47. Kasetsart University Annual Conference, Bangkok, Thailand, 17–20 March 2009.
33. Chang, W.H.; Chen, S.; Tsai, C.C. Development of a universal algorithm for use of nir in estimation of soluble solids in fruit juices. *Trans. ASAE* **1998**, *41*, 1739–1745. [CrossRef]
34. Theanjumpol, P.; Sardsud, V.; Self, G. Determination of characteristic absorption bands for carbohydrates and organic acids in mango purée. In *Proceedings of the 14th ICNIRS Conference, Bangkok, Thailand, 7–16 November 2009*; Saranwong, S., Kasemsumran, S., Thanapase, W., Eds.; Williams Racing: Wantage, UK, 2009; pp. 291–294.
35. Szuvandzsiev, P.; Helyes, L.; Lugasi, A.; Szántó, C.; Baranowski, P.; Pék, Z. Estimation of antioxidant components of tomato using VIS-NIR reflectance data by handheld portable spectrometer. *Int. Agrophys.* **2014**, *28*, 521–527. [CrossRef]
36. Cozzolino, D. Infrared Spectroscopy as a Versatile Analytical Tool for the Quantitative Determination of Antioxidants in Agricultural Products, Foods and Plants. *Antioxidants* **2015**, *4*, 482–497. [CrossRef]
37. Amodio, M.L.; Piazzolla, F.; Colantuono, F.; Colelli, G. The use of rapid FT-NIR methods to predict soluble solids, pH, titratable acidity and phenols of clingstone peaches ('Baby Gold 9'). In Proceedings of the VIII International Postharvest Symposium: Enhancing Supply Chain and Consumer Benefits-Ethical and Technological Issues 1194, Cartagena, Spain, 21–24 June 2016; pp. 1111–1118.
38. Downey, G.; Kelly, J.D. Detection and Quantification of Apple Adulteration in Diluted and Sulfited Strawberry and Raspberry Purées Using Visible and Near-Infrared Spectroscopy. *J. Agric. Food Chem.* **2004**, *52*, 204–209. [CrossRef]
39. Sitorus, A.; Lapcharoensuk, R. A Comprehensive Overview Of Near Infrared And Infrared Spectroscopy For Detecting The Adulteration On Food And Agroproducts—A Critical Assessment. *INMATEH-Agric. Eng.* **2022**, *67*, 465–486. [CrossRef]
40. Wold, S.; Sjöström, M.; Eriksson, L. PLS-regression: A basic tool of chemometrics. *Chemom. Intell. Lab. Syst.* **2001**, *58*, 109–130. [CrossRef]
41. Huang, Y. Linear Calibration Methods. In *Chemometric Methods in Analytical Spectroscopy Technology*; Chu, X., Huang, Y., Yun, Y., Bian, X., Eds.; Springer: Singapore, 2022. [CrossRef]
42. Romía, M.B.; Bernàrdez, M.A. Multivariate Calibration for Quantitative Analysis. In *Infrared Spectroscopy for Food Quality Analysis and Control*, 1st ed.; Sun, D.-W., Ed.; Academic Press: Cambridge, MA, USA, 2009.
43. Cho, S.; Chung, H.; Lee, Y. Simple and fast near-infrared spectroscopic analysis of hydroxyl number of polyol using a disposable glass vial. *Microchem. J.* **2005**, *80*, 189–193. [CrossRef]
44. Williams, P.; Antoniszyn, J.; Manley, M. *Near-Infrared Technology: Getting the Best Out of Light*; SUN PReSS: Stellenbosch, South Africa, 2019.
45. Saechua, W.; Sharma, S.; Nakawajana, N.; Leepaitoon, K.; Chunsri, R.; Posom, J.; Roeksukrungrueang, C.; Siritechavong, T.; Phanomsophon, T.; Sirisomboon, P.; et al. Integrating Vis-SWNIR spectrometer in a conveyor system for in-line measurement of dry matter content and soluble solids content of durian pulp. *Postharvest Biol. Technol.* **2021**, *181*, 111640. [CrossRef]
46. Posom, J.; Phuphanutada, J.; Lapcharoensuk, R. Gross calorific and ash content assessment of recycled sawdust from mushroom cultivation using near infrared spectroscopy. *MATEC Web Conf.* **2018**, *192*, 03021. [CrossRef]
47. Dardenne, P. Some considerations about NIR Spectroscopy: Closing Speech at NIR-2009. *NIR News* **2010**, *21*, 8–14. [CrossRef]
48. Sharma, S.; Sirisomboon, P. Precision test for spectral characteristic of on-line Vis-NIR versus at-line NIR spectroscopy for measuring total soluble solids of mango (Mangifera indica CV Nam Doc Mai). In Proceedings of the 10th TSAE International Conference (TSAE2017), IMPACT Exhibition and Convention Center, IMPACT FORUM 2, Bangkok, Thailand, 7–9 September 2017.
49. Srisawat, K.; Sirisomboon, P.; Pun, U.K.; Krusong, W.; Rakmae, S.; Chaomuang, N.; Mawilai, P.; Pongsuttiyakorn, T.; Chookaew, C.; Pornchaloempong, P. Temperature Difference in Loading Area (Tarmac) during Handling of Air Freight Operations and Distance of Production Area Affects Quality of Fresh Mango Fruits (*Mangifera indica* L.'Nam Dok Mai Si Thong'). *Horticulturae* **2022**, *8*, 1001. [CrossRef]
50. Palapol, Y.; Ketsa, S.; Stevenson, D.; Cooney, J.M.; Allan, A.C.; Ferguson, I.B. Colour development and quality of mangosteen (*Garcinia mangostana* L.) fruit during ripening and after harvest. *Postharvest Biol. Technol.* **2009**, *51*, 349–353. [CrossRef]
51. Osborne, B.G.; Fearn, T.; Hindle, P.H. *Practical NIR Spectroscopy with Applications in Food and Beverage Analysis*, 2nd ed.; Browning, D., Ed.; Longman Scientific and Technical: New York, NY, USA, 1993.
52. Theron, M.M.; Lues, J.F.R. Organic acids and meat preservation: A review. *Food Rev. Int.* **2007**, *23*, 141–158. [CrossRef]
53. Wang, H.; Peng, J.; Xie, C.; Bao, Y.; He, Y. Fruit quality evaluation using spectroscopy technology: A review. *Sensors* **2015**, *15*, 11889–11927. [CrossRef] [PubMed]
54. Workman, J., Jr.; Weyer, L. *Practical Guide to Interpretive Near-Infrared Spectroscopy*, 1st ed.; CRC Press: Boston, MA, USA, 2007.
55. Oliveira, G.A.; Castilhos, F.; Renard, C.M.G.C.; Bureau, S. Comparison of NIR and MIR spectroscopic methods for determination of individual sugars, organic acids and carotenoids in passion fruit. *Food Res. Int.* **2014**, *60*, 154–162. [CrossRef]
56. Xie, L.; Ye, X.; Liu, D.; Ying, Y. Prediction of titratable acidity, malic acid, and citric acid in bayberry fruit by near-infrared spectroscopy. *Food Res. Int.* **2011**, *44*, 2198–2204. [CrossRef]